

THE BACKWARD TW STRUCTURE FOR THE FERMI@ELETTRA LINAC*

C. Serpico, P. Craievich, C. Pasotti, Sincrotrone Trieste, Trieste, Italy

Abstract

The FERMI@Elettra project will use the existing ELETTRA linac. The linac includes seven accelerating sections. Each section is a backward traveling wave (BTW) structure comprised of 162 nose re-entrant cavities coupled magnetically. Furthermore, there are specialized input and output cavities specifically designed to match the structure to the RF source and load.

These BTW accelerating structures were designed by CGR MeV. That structures work on the $\frac{3}{4}\pi$ mode which was chosen to optimize the structure efficiency and to achieve a simple RF tuning setup. These sections are powered by a TH2132A 45 MW klystron providing a 4.5 μ s rf pulse and are coupled to a Thomson CIDR (Compresseur d'impulsion a Double Resonateur).

In this paper the $\frac{3}{4}\pi$ backward BTW structures are investigated and the results of electromagnetic and thermal simulations are presented.

INTRODUCTION

Each BTW accelerating section is a 6.15 m long structure made by 162 nose-cone cavities magnetically coupled [1, 2, 3]. In the following figure the structure geometry and the coupling slots are shown.

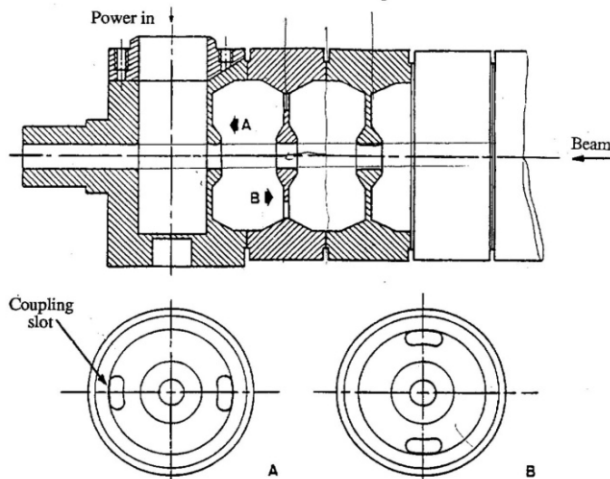


Figure 1: Section geometry with the input coupler and the coupling slots.

The group velocity is kept constant along the section by means of a constant geometry of the coupling slots; their surfaces and relative positioning have been chosen to get a c/v_g ratio equal to 38.

Moreover two different nose shape geometries have been used to optimize axial electrical field behaviour: the last 109 cells have been designed for a higher shunt

impedance value in order to compensate the attenuation along the structure.

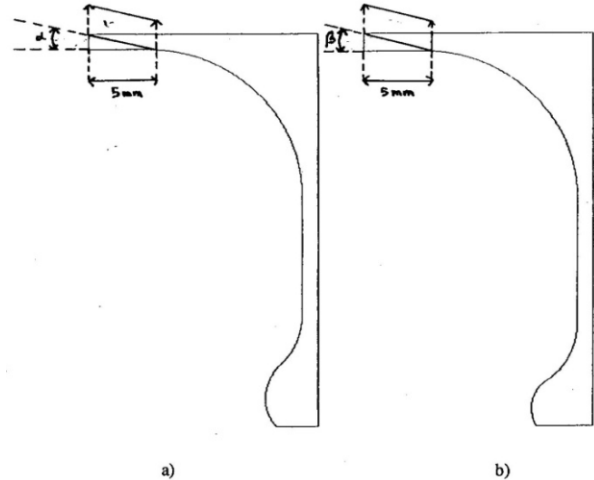


Figure 2: Geometry changes for multipacting effect: a) Low Peak Field cell; b) Medium Peak Field Cell.

The upper geometry of each cavity has been specially designed to avoid multipacting effects. Figure 2 shows the adopted solution for both kinds of cell.

Several simulations have been done by means of HFSS v.11 in order to verify the single cell and the whole section features. In the following the main results of the $\frac{3}{4}\pi$ backward BTW structures are presented. Other results are reported in [4].

LOW PEAK FIELD CELL

In Figure 3 it is shown the geometry of the cell simulated. In order to find the appropriate working mode, a 135 degree phase shift has been set up between the half cell planes.

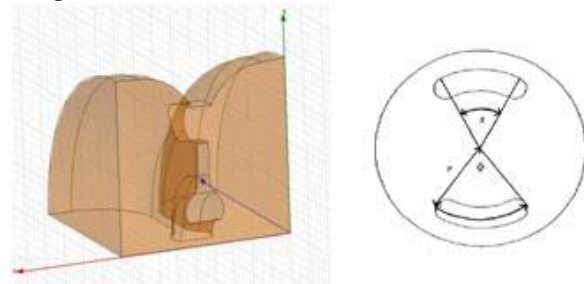


Figure 3: Geometry of the single cell.

Unfortunately, the exact cell shape and the magnetic coupling slot size are unknown.

The coupling slot angle θ is designed to reach $c/v_g=38$. During the first simulations, the θ value has been set as a variable parameter to fit the expected cell parameters.

The group velocity rises increasing the magnetic coupling angle θ . In the following table the results for the $\frac{3}{4}\pi$ mode are shown:

*Work supported by the Italian Ministry of University and Research under grants FIRB-RBAP045JF2 and FIRB-RBAP06AWK3

Table 1: Parametric analysis results

θ	35	37	39	41	43	45
f_0 [MHz]	3004.8	2996.5	2985.5	2974.4	2963.1	2951.1
Q	12855	12588	12164	11950	11632	11343
c/v_g	52.1	46.4	46	40.2	34.1	33.3

In order to have a group velocity close to the measured one we consider $\theta=41.4^\circ$. Using this value we obtain $c/v_g=38.1$. This value corresponds to $v_g=-7.86 \cdot 10^6$ m/s.

As we can see from the above table, the frequency we obtained doesn't match with the measured one. To have the right value of the working frequency it is necessary to consider the modified shape of the cavities as in the following picture.

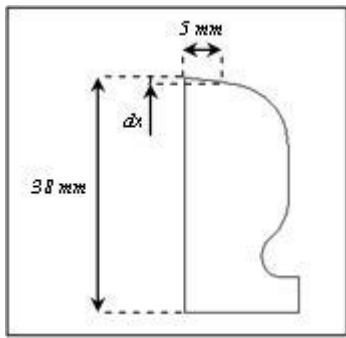


Figure 4: Modified shape designed to avoid multipacting effects.

As before, the exact shape is not known. We realized a parametric analysis by varying dx. If $dx=0.4$ mm, the frequency of the $3/4\pi$ mode is 2997.9 MHz. This value fits with the measured frequency.

Once we found the exact cell shape and the size of the magnetic coupling slots, we evaluate all the other electromagnetic parameters. Table 2 shows the results of the electromagnetic analysis. These results are compared with that obtained by CGR MeV and with the measured one.

Table 2: Low Peak Field Cell parameters

	CGR MeV	HFSS	S1(measured after brazing)
Angle θ [degree]		41.4	
f_0 [MHz]	2997.7	2997.9	2997.74
Q	12500	11775	11687
c/v_g	38	38.1	36.9
Z [M Ω /m]	77.4	71.1	
Z/Q	6195	6041	

The single cell shows another significant feature as the group velocity goes towards the requested value: the surface electric field on the magnetic coupling slot becomes of the same magnitude and even higher than the surface electric peak field on the nose.

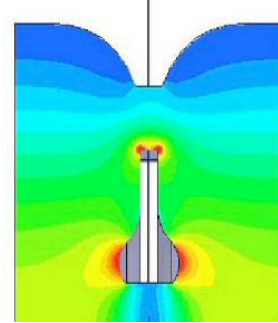


Figure 5: Electric field intensity.

Playing with the magnetic coupling slot sizes to reach the desired v_g , a significant peak electric field near the coupling slot arises. In particular the maximum electric peak on the surface of the first cell can be calculated by:

$$E_s [MV/m] = 9.4 \cdot \sqrt{P_{RF} [MW]} \quad (1)$$

where PRF is the RF power at the entrance of the accelerating section. Let us consider that the klystron output power is 40 MW and the pulse length is 4.5 μ s. By means of the Thomson CIDR, the RF klystron pulse of 4.5 μ s is compressed to 0.77 μ s to increase the available power from 40 MW to 150 MW rectangular equivalent (240 MW peak at the phase reversal-time). Considering these RF powers the maximum electric peaks on the surface of the first cell are 115MV/m and 146MV/m, respectively.

MEDIUM PEAK FIELD CELL

The last 109 cells have been designed with a different nose shape in order to have a higher shunt impedance value. The different nose shape compensates for the attenuation along the structure.

As before, the exact cell shape and the magnetic coupling slot size are unknown.

The first parametric analysis has been implemented by varying the coupling slot angle θ in order to fit the expected value of c/v_g . Such a value has been reached for $\theta=41.4^\circ$.

Again, the frequency we obtained doesn't match with the measured one.

Let us now consider the modified shape of the cavities. A new analysis has been realized by varying the geometric parameter dx. Since the nose shape is more pronounced than the one of the first cell type, it is necessary to have an higher value of dx in order to have the same working frequency. In this case, if $dx=0.7$ mm the frequency fits the measured one.

As before, once we found the exact cell shape and the size of the magnetic coupling slots, we evaluate all the other electromagnetic parameters. The following table shows the results of the electromagnetic analysis.

Table 3: Medium Peak Field Cell parameters

	CGR MeV	HFSS
Angle θ [degree]		41.4
f_0 [MHz]	2997.7	2997
Q	12500	11723
c/v_g	38	38.8
Z [M Ω /m]	81	72.9
Z/Q	6485	6218

PULSED HEATING

Average heating and pulse heating are typically the two types of heating effects that are taken into account in pulsed systems.

A steady-state thermal analysis is useful for determining the average stresses on the copper structure. From this one can determine whether the stresses have exceeded the yield strength and have potentially compromised the material. Of course, this information is also useful in determining cavity frequency shift.

On the other hand, pulse heating is a transient event and therefore more difficult to characterize. It creates a momentary thermal "surge" at local points in the cavity geometry that is not considered in the steady-state calculation. If pulse heating is excessive, surface crazing may occur which will degrade the cavity surface quality and RF performance.

A transient thermal analysis has been carried out by means of Ansys Multiphysics. Since the structure is a BTW, the dissipated power exponentially decays along the z-direction. So, in order to evaluate the maximum temperature rise due to the pulsed heating phenomena, it is sufficient to consider the first cell of the BTW accelerating structure.

Figure 6 show the thermal profile of the first accelerating cell due to the pulse heating phenomena.

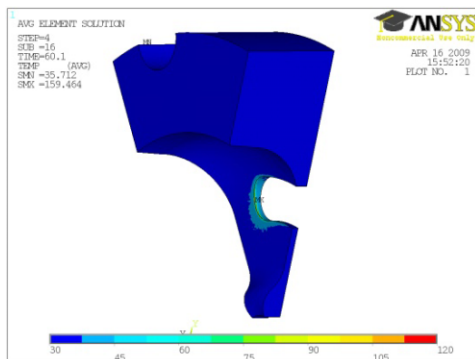


Figure 6: Thermal profile due to pulse heating.

As it is pointed out in the previous picture, the maximum temperature is achieved on the coupling slots where the magnetic field is stronger.

During the RF pulse, on the edge of the coupling slots the temperature reaches 120 °C. A more detailed view is shown in the next figure.

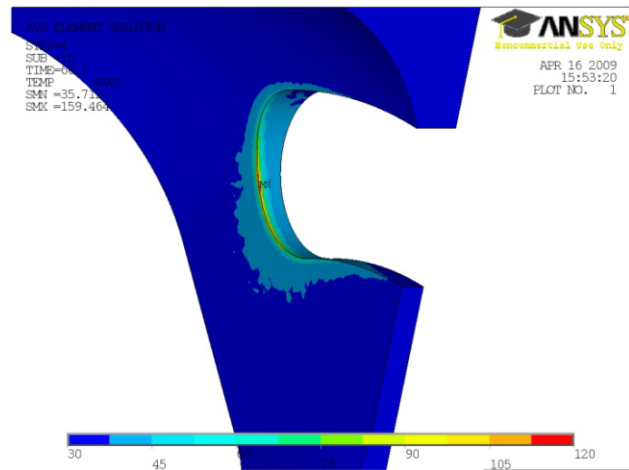


Figure 7: Thermal profile on the magnetic coupling slot.

According to a rule-of-thumb, pulse heating effects should not exceed 50 °C. If pulse heating is excessive, the cavity surface quality could be corrupted. As a consequence RF performance will degrade.

Starting from the results of the transient thermal analysis it is clear that the temperature rise on the coupling slots is above the empirical limit of 50 °C. As it is shown in the previous pictures, the temperature reaches 120 °C on the edge of the coupling slots

CONCLUSION

In this paper the $\frac{3}{4}\pi$ backward BTW accelerating structures for the FERMI@ELETTRA project have been investigated. The electromagnetic simulations on BTW structures verified that cell's and section's features fit the measured parameters. It is worthwhile noting that the electric field on the surface of the first cell is 146MV/m when an RF input power of 240MW is used.

Pulse heating phenomena have also been studied. It has been pointed out that the temperature rises up to 120 °C during the RF pulses. According to a rule-of-thumb, pulse heating effects should not exceed 50 °C. Due to the excessive heating, surface crazing may occur which could degrade the cavity surface quality and RF performance.

REFERENCES

- [1] G. D'Auria and C. Rossi, "RF Measurements on the First Backward TW of the Trieste 2 Linac", Elettra Internal technical note ST/M-TN-91/15, 1991.
- [2] P. Girault, "The $\frac{3}{4}\pi$ Backward TW Structure for the ELETTRA 1.5 GeV Electron Injector", General Electric CGR MeV, Proceeding of the IEEE PAC, San Francisco 1991.
- [3] P. Girault et al., "Progress report on $\frac{3}{4}\pi$ Backward TW Accelerating Module for the ELETTRA 1.5 GeV Electron Injector", Proceeding of the first EPAC, pp.518-520, Rome 1992.
- [4] C. Pasotti and P. Craievich, "Numerical Simulation of the Backward Traveling Wave LINAC Type I Cell", FERMI Internal talk, November 2008